arXiv:1611.01849v1 [physics.soc-ph] 6 Nov 2016

Universal structural estimator and dynamics approximator for complex networks

Yu-Zhong Chen[1] and Ying-Cheng Lai[1,2,*]

[1]*School of Electrical, Computer and Energy Engineering, Arizona State University, Tempe, Arizona 85287, USA*

[2]*Department of Physics, Arizona State University, Tempe, Arizona 85287, USA*

Abstract

Revealing the structure and dynamics of complex networked systems from observed data is of fundamental importance to science, engineering, and society. Is it possible to develop a universal, completely data driven framework to decipher the network structure and different types of dynamical processes on complex networks, regardless of their details? We develop a Markov network based model, sparse dynamical Boltzmann machine (SDBM), as a universal network structural estimator and dynamics approximator. The SDBM attains its topology according to that of the original system and is capable of simulating the original dynamical process. We develop a fully automated method based on compressive sensing and machine learning to find the SDBM. We demonstrate, for a large variety of representative dynamical processes on model and real world complex networks, that the equivalent SDBM can recover the network structure of the original system and predicts its dynamical behavior with high precision.

* Ying-Cheng.Lai@asu.edu

I. INTRODUCTION

A central issue in complexity science and engineering is systems identification and dynamical behavior prediction based on experimental or observational data. For a complex networked system, often the network structure and the nodal dynamical processes are unknown but only time series measured from various nodes in the network can be obtained. The challenging task is to infer the detailed network topology and the nodal dynamical systems from the available data. This line of pursuit started in biomedical science for problems such as identification of gene regulatory networks from expression data in systems biology [1–4] and uncovering various functional networks in the human brain from activation data in neuroscience [5–8]. The inverse problem has also been an area of research in statistical physics where, for example, the inverse Ising problem in static [9–13] and kinetic [14–20] situations has attracted continuous interest. Recent years have witnessed the emergence and growth of a subfield of research in complex networks: data based network identification (or reverse engineering of complex networks) [21–29]. In these works, the success of mapping out the entire network structure and estimating the nodal dynamical equations partly relies on taking advantage of the particular properties of the system dynamics in terms of the specific types and rules. For example, depending on the detailed dynamical processes such as continuous-time oscillations [26, 30, 31], evolutionary games [27], or epidemic spreading [28], appropriate mathematical frameworks uniquely tailored at the specific underlying dynamical process can be formulated to solve the inverse problem.

In this paper, we address the following challenging question: is it possible to develop a universal and completely data-driven framework for extracting network topology and identifying the dynamical processes, without the need to know a priori the specific types of network dynamics? An answer to this question would be of significant value not only to complexity science and engineering but also to modern data science where the goal is to unearth the hidden structural information and to predict the future evolution of the system. Here we introduce the concept of *universal structural estimator and dynamics approximator* for complex networked systems and demonstrate that such a framework or "machine" can indeed be developed for a large number of distinct types of network dynamical processes. Our approach will be a combination of numerical computation and physical reasoning. Since we are yet able to develop a rigorous mathematical framework, the present work should be regarded as an initial attempt towards the development of a universal framework for network reconstruction and dynamics prediction.

The key principle underlying our work is the following. In spite of the difference among the types of dynamics in terms of, e.g., the interaction patterns and state updating rules, there are two common features shared by many dynamical processes on complex networks: (1) they are stochastic, first-order Markovian processes, i.e., only the current state of the system determines its immediate future; and (2) the nodal interactions are local, i.e., a node typically interacts with its neighboring nodes, not all the nodes in the network. The two features are characteristic of a *Markov network* (or a *Markov random field*) [32, 33]. In particular, a Markov network is an undirected and weighted probabilistic graphical model that is effective at determining the complex probabilistic interdependencies in situations where the directionality in the interaction between connected nodes cannot be naturally assigned, in contrast to the directed Bayesian networks [32, 33]. A Markov network has two types of parameters: a

nodal bias parameter that controls its preference of the state choice, and a weight parameter characterizing the interaction strength of each undirected link. For a network of N nodes with x_j being the state of node j ($j = 1, \ldots, N$), the joint probability distribution of the state variables $\mathbf{X} = (x_1, x_2, \ldots, x_N)^{\mathrm{T}}$ is given by $P(\mathbf{X}) = \prod_C \phi(\mathbf{X}_C) / \sum_{\mathbf{X}} \prod_C \phi(\mathbf{X}_C)$, where $\phi(\mathbf{X}_C)$ is the potential function for a well-connected network clique C, and the summation in the denominator is over all possible system state $\mathbf{X}$. If this joint probability distribution is available, all conditional probability interdependencies can be obtained. The way to define a clique and to determine its potential function plays a key role in the Markov network's representation power of modeling the interdependencies within a particular system.

To be concrete, in this work we pursue the possibility of modeling the conditional probability interdependencies of a variety of dynamical processes on complex networked systems via a binary Ising Markov network with its potential function in the form of the Boltzmann factor, $\exp(-E)$, where E is the energy determined by the local states and their interactions along with the network parameters (the link weights and node biases) in a *log-linear* form [34]. This is effectively a sparse Boltzmann machine [34] adopted to complex network topologies without hidden units. (Note that hidden units usually play a crucial role in ordinary Boltzmann machines [34]). We introduce a temporal evolution mechanism as a persistent sampling process for such a machine based on the conditional probabilities obtained via the joint probability, and generate a Markov chain of persistently sampled state configurations to form the state transition time series for each node. We call our model a *sparse dynamical Boltzmann machine* (SDBM).

For a dynamical process on complex networks, such as epidemic spreading or evolutionary game dynamics, the state of each node at the next time step is determined by the probability conditioned on the current states of its neighbors (and its own state in some cases). There is freedom to manipulate the conditional probabilities that dictate the system behavior in the immediate future by adjusting the values of its parameters, i.e., the weights and biases. A basic question is then, for an SDBM, is it possible to properly choose these parameters so that the conditional probabilities so produced are identical or nearly identical to those of the network dynamical process with each given observed system state configuration? If the answer is affirmative, the SDBM can serve as a dynamics approximator of the original system, and the approximated conditional probabilities possess predictive power for the system state at the next time step. When such an SDBM is found for many types of dynamical process on complex networks, it effectively serves as a universal dynamics approximator. Moreover, if the detailed statistical properties of the state configurations can be reproduced in the long time limit, that is, if the time series generated by this SDBM are statistically identical or nearly identical to those from the original system, then the SDBM will be a generative model of the observed data (in the language of machine learning), which is potentially capable of long term prediction.

When a dynamics approximator exists for the dynamics on a complex network, the topology of the SDBM is nothing but that of the original network, providing a simultaneous solution to the problem of network structure reconstruction. Previous works on the inverse static or kinetic Ising problems led to methods of reconstruction for Ising dynamics by maximizing the data likelihood (or pseudo-likelihood) function via the gradient descent approaches [9–20]. Instead of adopting these approaches, as a part of our methodology to extract the network structure, we articulate a compressive sensing [35–40] based approach,

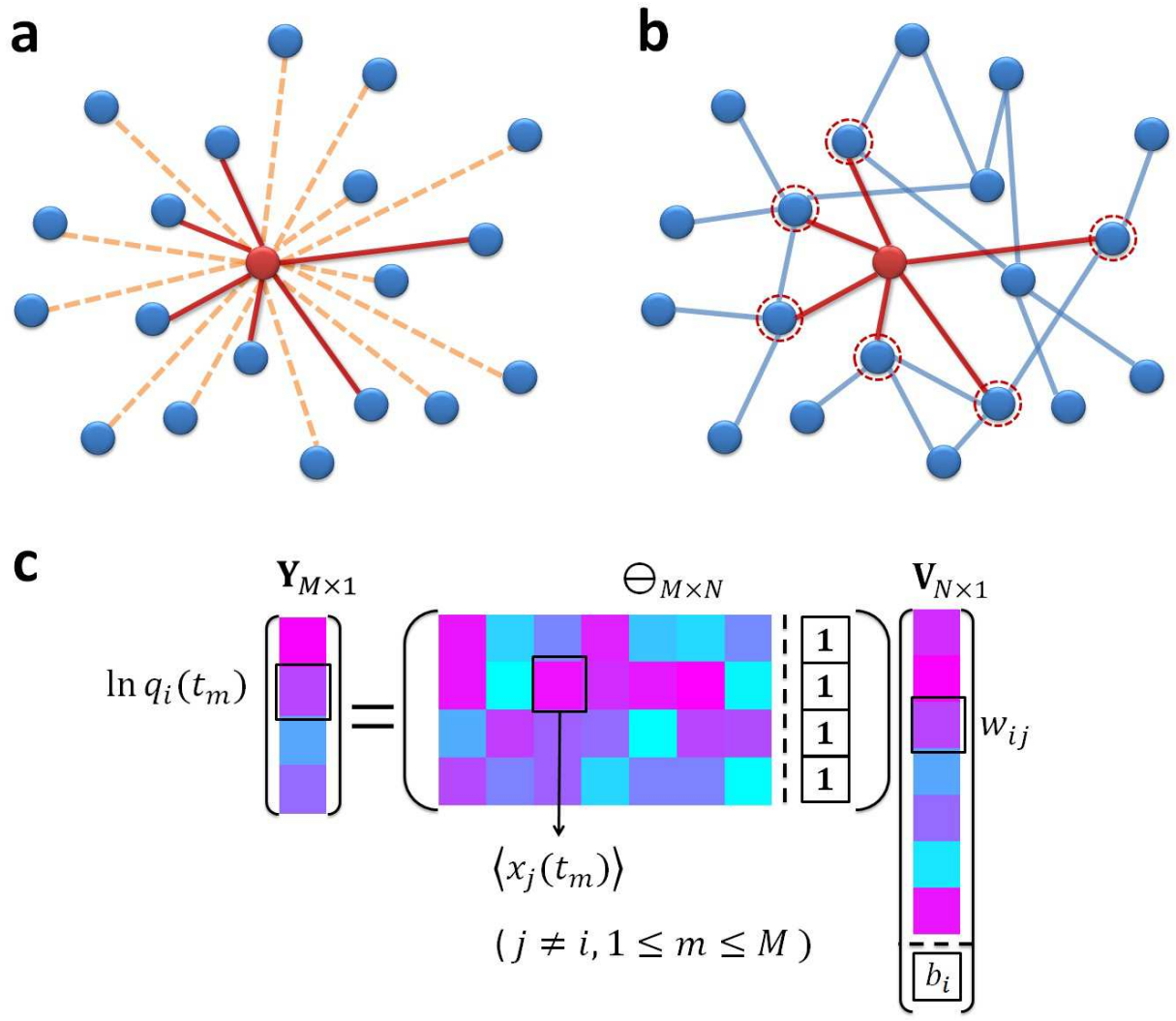

FIG. 1: A schematic illustration of reconstruction of network structure using SDBM. (a) Reconstruction of the local connection structure of the red node in a network of 20 nodes. The connections of the network are assumed to be unknown, so the red node can potentially be connected with any other node, as shown by the orange dashed links. Executing compressive sensing [(c)] and the K-means clustering [Fig.6] for this node based on time series leads to its true connection structure, marked by the red links. The link weights and the nodal bias are represented by the vector $\mathbf{V}_{N\times 1}$ in (c). (b) All true connections of the network are recovered through the process in (a) for each node. The Markov blanket of the red node in (a) consists of all its nearest neighbors, indicated by the nodes with dashed red circles. (c) A schematic illustration of the compressive sensing framework for structural reconstruction as in Eq. (9).

whose working power has been demonstrated for a variety types of non-Ising type of dynamics on complex networks [26–29, 41–43]. By incorporating the K-means clustering algorithm into the sparse solution obtained from compressive sensing, we demonstrate that nearly perfect reconstruction of the complex network topology can be achieved. Using 14 different types of dynamical processes on complex networks, we find that, if the time series data generated by these dynamical processes are assumed to be from its equivalent SDBMs, the

universal reconstruction framework is capable of recovering the underlying network structure for each type of original dynamics with practically zero error. This represents solid and concrete evidence that SDBM is capable of serving as a universal structural estimator for complex networks. In addition to being able to precisely reconstruct the network topology, the SDBM also allows the link weights and nodal biases to be calculated with high accuracy.

Our method is fully automated and does not require any subjective parameter choice.

II. RESULTS

A. SDBM as a network structural estimator

For an SDBM of size N, the probability that the system is in a particular binary state configuration $\mathbf{X}_{N\times 1} = (x_1, x_2, \ldots, x_N)^{\mathrm{T}}$ is given by

$$P(\mathbf{X}) = \frac{\exp(-E_{\mathbf{X}})}{\sum_{\mathbf{X}} \exp(-E_{\mathbf{X}})}, \tag{1}$$

where $E_{\mathbf{X}}$ is the total energy of the network in $\mathbf{X}$:

$$E_{\mathbf{X}} = \mathbf{X}^{\mathrm{T}} \cdot \mathbf{W} \cdot \mathbf{X} = \sum_{i=1, i\neq j}^{N} \sum_{j=1, j\neq i}^{N} w_{ij} x_i x_j - \sum_{i=1}^{N} b_i x_i, \tag{2}$$

x_i and x_j are binary variables (0 or 1) characterizing the states of nodes i and j, respectively, and $\mathbf{W}$ is a weighted matrix with its off diagonal elements $w_{ij} = w_{ji}$ $(i, j = 1, \ldots, N,\ i \neq j)$ specifying the weight associated with the link between nodes i and j. The ith diagonal element of $\mathbf{W}$ is the bias parameter b_i for node i $(i = 1, \ldots, N)$, which determines node i's preference to state 0 or 1. The total energy $E_{\mathbf{X}}$ includes the interaction energies (the sum of all $w_{ij}x_ix_j$ terms) and the nodes' self energies (the various b_ix_i terms). The partition function of the system is given by

$$\mathcal{Z} = \sum_{\mathbf{X}} \exp(-E_{\mathbf{X}}), \tag{3}$$

where the summation is over all possible $\mathbf{X}$ configurations. The state of node i at the next time step is determined by the states of all the other nodes at the present time step, $\mathbf{X}_i^{\mathrm{R}}$, through the following conditional probability

$$P\{x_i(t+1) = 1 | \mathbf{X}_i^{\mathrm{R}}(t)\} = \frac{P\{x_i(t+1) = 1, \mathbf{X}_i^{\mathrm{R}}(t)\}}{P\{x_i(t+1) = 1, \mathbf{X}_i^{\mathrm{R}}(t)\} + P\{x_i(t+1) = 0, \mathbf{X}_i^{\mathrm{R}}(t)\}}, \tag{4}$$

where the two joint probabilities are given by

$$P\{x_i(t+1) = 1, \mathbf{X}_i^{\mathrm{R}}(t)\} = \frac{1}{\mathcal{Z}} \exp\Big[-\sum_{j=1, j\neq i}^{N} w_{ij} x_j(t) - b_i - \sum_{s=1, s\neq i}^{N} \sum_{j=1, j\neq i}^{N} w_{sj} x_s(t) x_j(t) - \sum_{s=1, s\neq i}^{N} b_s x_s(t)\Big],$$

$$P\{x_i(t+1) = 0, \mathbf{X}_i^{\mathrm{R}}(t)\} = \frac{1}{\mathcal{Z}} \exp\Big[-\sum_{s=1, s\neq i}^{N} \sum_{j=1, j\neq i}^{N} w_{sj} x_s(t) x_j(t) - \sum_{s=1, s\neq i}^{N} b_s x_s(t)\Big].$$

A Markov network defined in this fashion is in fact the kinetic Ising model [14–20]. With the joint probabilities, the conditional probability in Eq. (4) becomes

$$P\{x_i(t+1)=1|\mathbf{X}_i^{\mathrm{R}}(t)\}=\frac{1}{1+\exp\left[\sum_{j=1,j\neq i}^{N}w_{ij}x_j(t)+b_i\right]}. \tag{5}$$

We thus have

$$\ln\left(\frac{1}{P\{x_i(t+1)=1|\mathbf{X}_i^{\mathrm{R}}(t)\}}-1\right)=\sum_{j=1,j\neq i}^{N}w_{ij}x_j(t)+b_i.$$

Letting $Q_i(t)\equiv\left(P\{x_i(t+1)=1|\mathbf{X}_i^{\mathrm{R}}(t)\}\right)^{-1}-1$, we have

$$\ln Q_i(t)=\left(\begin{array}{ccccccc} x_1(t), & \ldots, & x_{i-1}(t), & x_{i+1}(t), & \ldots, & x_N(t), & 1 \end{array}\right)\left(\begin{array}{c} w_{i1} \\ \vdots \\ w_{i(i-1)} \\ w_{i(i+1)} \\ \vdots \\ w_{iN} \\ b_i \end{array}\right) \tag{6}$$

For M distinct time steps $t_1, t_2, \ldots, t_M$, we obtain the following matrix form:

$$\left(\begin{array}{c} \ln Q_i(t_1) \\ \ln Q_i(t_2) \\ \vdots \\ \ln Q_i(t_M) \end{array}\right)=\left(\begin{array}{ccccccc} x_1(t_1), & \ldots, & x_{i-1}(t_1), & x_{i+1}(t_1), & \ldots, & x_N(t_1), & 1 \\ x_1(t_2), & \ldots, & x_{i-1}(t_2), & x_{i+1}(t_2), & \ldots, & x_N(t_2), & 1 \\ \vdots & & \vdots & \vdots & & \vdots & \vdots \\ x_1(t_M), & \ldots, & x_{i-1}(t_M), & x_{i+1}(t_M), & \ldots, & x_N(t_M), & 1 \end{array}\right)\left(\begin{array}{c} w_{i1} \\ \vdots \\ w_{i(i-1)} \\ w_{i(i+1)} \\ \vdots \\ w_{iN} \\ b_i \end{array}\right), \tag{7}$$

which can be written concisely as

$$\mathbf{Y}_{M\times 1}=\ominus_{M\times N}\cdot\mathbf{V}_{N\times 1}, \tag{8}$$

where the vector $\mathbf{Y}_{M\times 1}\in R^M$ contains the values of $\ln Q_i(t)$ for M different time steps, the $M\times N$ matrix $\ominus_{M\times N}$ is determined by the states of all the nodes except i, and the first $(N-1)$ components of the vector $\mathbf{V}_{N\times 1}\in R^N$ are the link weights between node i and all other nodes in the network, as illustrated in Fig. 1(a), with its last entry being node i's intrinsic bias.

Since, as shown in Fig. 1(b), the conditional probability $P\{x_i(t+1)=1|\mathbf{X}_i^{\mathrm{R}}(t)\}$ depends solely on the state configuration of i's nearest neighbors, or i's *Markov blanket* [32, 33] at time t, identical configurations at other time steps imply identical conditional probabilities. Thus, given time series data of the dynamical process, the conditional probability can be estimated according to the law of large numbers by averaging over the states of i at all the time steps prior to the neighboring state configurations becoming identical. Note, however,

that this probability needs to be conditioned on the state configuration of the entire system except node i, i.e., on $\mathbf{X}_i^{\mathrm{R}}(t)$, and the average of x_i is calculated over all the time steps t_m+1 satisfying $\mathbf{X}_i^{\mathrm{R}}(t) = \mathbf{X}_i^{\mathrm{R}}(t_m)$. This means that there can be a dramatic increase in the configuration size, i.e., from k_i (the degree of node i) to $N-1$ (the size of the vector $\mathbf{X}_i^{\mathrm{R}}$), which can make the number of exactly identical configurations too small to give any meaningful statistics. To overcome this difficulty, we allow a small amount of dissimilarity between $\mathbf{X}_i^{\mathrm{R}}(t)$ and $\mathbf{X}_i^{\mathrm{R}}(t_m)$ by introducing a tolerance parameter, Γ, to confine the corresponding Hamming distances normalized by N. In particular, we assume $\mathbf{X}_i^{\mathrm{R}}(t) \approx \mathbf{X}_i^{\mathrm{R}}(t_m)$ if the relative difference between them is not larger than Γ/N. This averaging process leads to

$$\begin{pmatrix} \ln q_i(t_1) \\ \ln q_i(t_2) \\ \vdots \\ \ln q_i(t_M) \end{pmatrix} = \begin{pmatrix} \langle x_1(t_1)\rangle, & \ldots, & \langle x_{i-1}(t_1)\rangle, & \langle x_{i+1}(t_1)\rangle, & \ldots, & \langle x_N(t_1)\rangle, & 1 \\ \langle x_1(t_2)\rangle, & \ldots, & \langle x_{i-1}(t_2)\rangle, & \langle x_{i+1}(t_2)\rangle, & \ldots, & \langle x_N(t_2)\rangle, & 1 \\ \vdots & & \vdots & \vdots & & \vdots & \vdots \\ \langle x_i(t_M)\rangle, & \ldots, & \langle x_{i-1}(t_M)\rangle, & \langle x_{i+1}(t_M)\rangle, & \ldots, & \langle x_N(t_M)\rangle, & 1 \end{pmatrix} \begin{pmatrix} w_{i1} \\ \vdots \\ w_{i(i-1)} \\ w_{i(i+1)} \\ \vdots \\ w_{iN} \\ b_i \end{pmatrix} \quad (9)$$

where $q_i(t) \equiv \langle x_i(t_1+1)\rangle^{-1} - 1$, with $\langle\cdot\rangle$ standing for the averaging over all instants of time at which the condition $\mathbf{X}_i^{\mathrm{R}}(t) = \mathbf{X}_i^{\mathrm{R}}(t_m)$ is met. A schematic illustration of the whole process is presented in Fig. 1, with Eq. (9) shown in panel (c).

For a complex network, the degree of a typical node is small compared with the network size. For node i, the link weights are nonzero only for the connections with the immediate neighbors. The vector $\mathbf{V}_{N\times 1}$ is thus typically sparse with the majority of its elements being zero. The sparsity property renders applicable compressive sensing [35–40], through which an N dimensional sparse vector can be reconstructed via a set of M measurements, for $M \ll N$. By minimizing the L_1 norm of $\mathbf{V}_{N\times 1}$, i.e., $\|\mathbf{V}_{N\times 1}\|_1 = \sum_{j=1,j\neq i}^{N} |w_{ij}| + |b_i|$, subject to the constraint $\mathbf{Y}_{M\times 1} = \ominus_{M\times N} \cdot \mathbf{V}_{N\times 1}$, we can reconstruct $\mathbf{V}_{N\times 1}$ to obtain the connection weights between node i and all other nodes in the network. One tempts to hope that, applying the procedure to each node would lead to the complete weighted adjacency matrix, $\mathbf{W}$.

To gain insights, we test the structural estimation method for an SDBM itself [Figs. 2(a-c)] and three different types of dynamical processes [Figs. 2(d-f)] by feeding the time series data generated by the SDBM into the framework and comparing the reconstructed SDBM with the original machine. The time instants $t_1, t_2, \ldots, t_M$ needed to construct Eq. (9) are chosen randomly from T time instants in total. For each node, compressive sensing is implemented a multiple of times to obtain the averaged relevant quantities. As shown in Fig. 2, the averaged solutions from the compressive sensing algorithm appear in sharp peaks at places that correspond to the existent links, despite the large differences among the values. This means that, while most existent links can be predicted against the null links, the accuracy of the solution so obtained is not sufficient for the actual element values of $\mathbf{V}_{N\times 1}$ to be determined. For the null links, the corresponding solutions generally appear as a noisy background. For the ideal case where w_{ij} is zero, the background noise can be quite large especially for the large degree nodes, as shown in Figs. 2(b) and 2(d). Further calculations

indicate that averaging a larger number of simulation runs can suppress the background noise to certain extent, but it cannot be eliminated and may become quite significant for various types of dynamics (Sec. II B).

In previous works on reconstruction of complex networks based on stochastic dynamical correlations [30, 31] or compressive sensing [27, 28], the existent (real) links can be distinguished from the nonexistent links by setting a single threshold value of certain quantitative measure. The success relies on the fact that the dynamics at various nodes are of the same type, and the reconstruction algorithm is tailored toward the specific type of dynamical process. Our task is significantly more challenging as the goal is to develop a universal system (or machine) to replicate a diverse array of dynamical processes based on data. As can be seen from Figs. 2(a-c), for compressive sensing based reconstruction, the computational criteria to distinguish existent from nonexistent links differ substantially for different dynamics in terms of quantities such as the solution magnitude, peak value distribution, and background noise intensity. As a result, a more elaborate and sophisticated procedure is required for determining the threshold for each particular case, suggesting that a straightforward application of compressive sensing cannot lead to a universal reconstruction algorithm. One may also regard the solutions of the existent links as a kind of *extreme events* [44–46] superimposed on top of the random background, but it is difficult to devise a universal criterion to determine if a peak in the distribution of the quantitative measure represents the correct extreme event corresponding to an existent link.

Through extensive testing, we find that a previously developed unsupervised clustering measure, the K-means [32, 33], possesses the desired traits that can be exploited, in combination with compressive sensing, to develop a universal reconstruction machine (see **Methods** for details). As we will show, K-means can serve as a base for a highly effective structural estimator for various types of dynamics on networks of distinct topologies. Depending on the specific combination of the network topology and dynamics, the reconstruction accuracies vary to certain extent but are acceptable. Since the compressive sensing operation is node specific, the solutions obtained separately from different nodes may give conflicting information as to whether there is an actual link between the two nodes, requiring a proper resolution scheme. We develop such a scheme based on node degree consistency (see **Methods**). Our universal reconstruction machine thus contains three main components: compressive sensing, K-means, and conflict resolution. We shall demonstrate that the machine can separate the true positive solutions from the noisy background with high success rate, for all combinations of the nodal dynamics and the network topology tested.

B. Universality of SDBM as a network structural estimator

Figure 3 demonstrates the performance of network structural estimation for SDBM dynamics on random and scale-free networks in terms of the data amount, characterized by the number of measurements M normalized by N, for SDBMs built up for systems with different original topologies. We define $R_{\rm e}^1$ and $R_{\rm e}^0$ as the estimation error rates for the existent and non-existent links, namely, the false positive and the false negative rates, respectively. We see that, for a wide range of the values of M/N, the success rates of the existent and non-existent links, $1-R_{\rm e}^1$ and $1-R_{\rm e}^0$, respectively, are nearly 100% for homogeneous network topology. For heterogeneous (scale-free) networks, the success rate $1-R_{\rm e}^1$ tends to be slightly

lower than 100%, due to the violation of the sparsity condition for hub nodes, leading to the difficulty to distinguish the peaks in the distribution of the compressive sensing solutions from the noisy background. For $M/N = 1$, the success rates are reduced slightly, due to the non-zero dissimilarity tolerance Γ that makes the values of $\mathbf{X}_i^{\mathrm{R}}$ at different time steps indistinguishable and introduces linear dependence into Eq. (9). As a result, the accuracy of compressive sensing solutions is compromised to certain extent. Generally, high reconstruction precision is guaranteed for almost any choice of M insofar as it is not too close to 0 and N, and this feature makes our SDBM framework free of any subjective parameters.

Our working hypothesis is that, for a networked system with a certain type of nodal dynamics, there exists an equivalent SDBM. Reconstructing the structure of the SDBM would simultaneously give the topology of the original networked dynamical system. Accordingly, the time series data generated from the original system can be used to reveal its underlining interaction structures through the corresponding SDBM. In particular, we directly feed the original time series into the framework of compressive sensing and K-means for SDBM to generate the network structure, and test whether the structure generated by the SDBM based reconstruction represents that of the original network. The similarity can be quantified by the error rates of the existent and non-existent links. Table I list the 14 dynamical processes on model networks and the underlying conditional probabilities, and Tab. II shows the performance in terms of the percentage error rates R_{e}^0 and R_{e}^1. The 14 types of dynamical processes are taken from the fields of evolutionary game theory, opinion dynamics, and spreading processes, covering a number of focused research topics in complex networks. Strikingly, for all the dynamics with diverse properties, we find that that, for each and every dynamics-network combination, zero or nearly zero error rates are obtained for both the existent and non-existent links, revealing a strong similarity between the original networks and the ones generated from SDBM, regardless of the type of dynamics. The nonzero error rates in Tab. II come mainly from the high degree nodes. Consequently, as indicated in Tab. II, the reconstruction accuracy for networks of homogeneous topology is generally higher than that for heterogeneous networks.

For certain types of evolutionary game dynamics, especially for the snowdrift game (SG) [68] and the prisoner's dilemma game (PDG) [69, 70] with the Fermi updating rule [70], information about the state configuration of the second nearest neighbors is required to calculate the payoffs of the first nearest neighbors. In such a system, the next move of a target node is determined by comparing its payoff with those of its neighbors. This implies that, using solely the state configuration information of the Markov blanket, without the aid of the payoff information that requires the state information of the second nearest neighbors, is insufficient to determine the state of the target node into the immediate future, rendering inapplicable our SDBM based reconstruction. Contrary to this intuition, we find that for both SG and PDG, high reconstruction accuracy can be achieved, as shown in Tab. II. Recall that our reconstruction method is formulated based on the independence assumption of Markov networks, i.e., in order to reconstruct the local structure of a target node, it should be completely independent of the rest of the system when the configuration of its Markov blanket is given. The results in Tab. II indicate that our SDBM based algorithm performs better than expected in terms of the reconstruction accuracy. In fact, the independence assumption can be made to hold by adopting a self-questioning (SQ) based updating rule (see Supplementary Note 1 for details). In this case, excellent reconstruction accuracy is

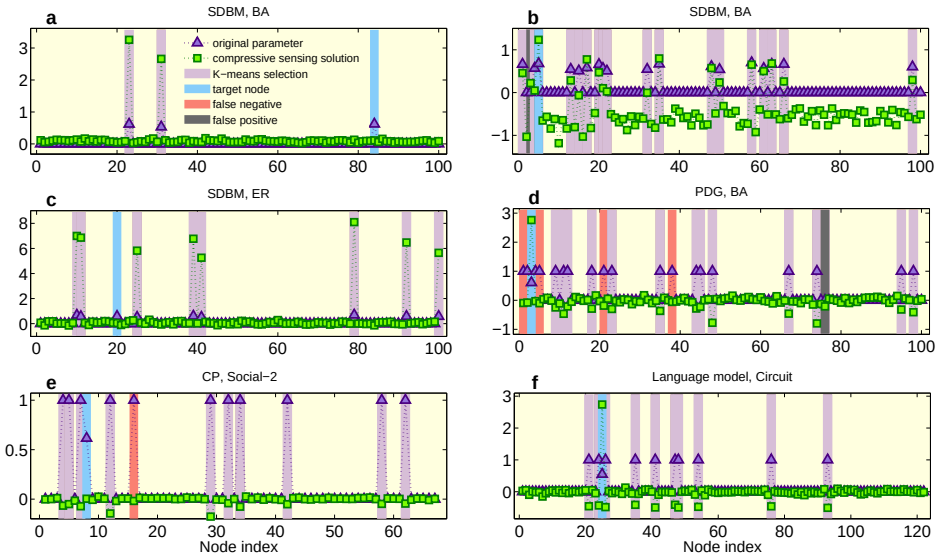

FIG. 2: Solution examples of compressive sensing and K-means clustering results. The compressive sensing solutions (green squares) are compared, element-wise, with the true values of the original connection vectors (dark purple triangles), where the x-axis is the index of nodes with different degree values for different network topologies and dynamics types. The target nodes and the correctly detected existent connections via the K-means are marked as light blue and light purple bars, respectively. The false negative and the false positive estimations are marked as red and gray bars, respectively. For all cases, the measurement amount is $M = 0.4N$. The restriction on Hamming distances is set to be $\Gamma = 0.35$ for all examples, and a small change in Γ would not affect the qualitative results. (a) A node with the smallest degree $k = 2$ in a BA scale-free network of size $N = 100$ and average degree $\langle k \rangle = 4$ with SDBM dynamics. (b) The node of the largest degree $k = 18$ in the same network. (c) A node of degree $k = 8$ in an ER random network of size $N = 100$ and average degree $\langle k \rangle = 4$ with SDBM dynamics. (d) The node with the largest degree $k = 19$ in a BA scale-free network of size $N = 100$ and average degree $\langle k \rangle = 4$ with prisoner's dilemma game (PDG) dynamics. (e) A node of degree $k = 11$ in a real world social network of size $N = 67$ subject to CP dynamics. (f) A node of degree $k = 10$ in a real world electrical circuit network of size $N = 122$ with Language model dynamics. In (d-f), the element values of the original connection vector are set to unity since no true weight values are given. For cases (a,b,c,f), there are no false negative detections, i.e., all existent links have been successfully detected. For cases (a,c,e), there are no false positive detections, i.e., no non-existent links are mistaken as existent ones. A detailed description of the dynamical processes is given in Tab. I.

obtained, as can be seen from Tab. II.

The structural estimation results reported so far are based on model network topologies. Real world complex networks have also been used to test our framework, with results shown in Figs. 2(e,f) and Supplementary Notes 2 and 3. For various combinations of the network topology and dynamical process, high reconstruction accuracy is achieved, where for a number of cases the error rates are essentially zero. There are a few special cases where the errors are relatively large, corresponding to situations where the globally frozen or oscillating states dominate the dynamical process so that too few linearly independent

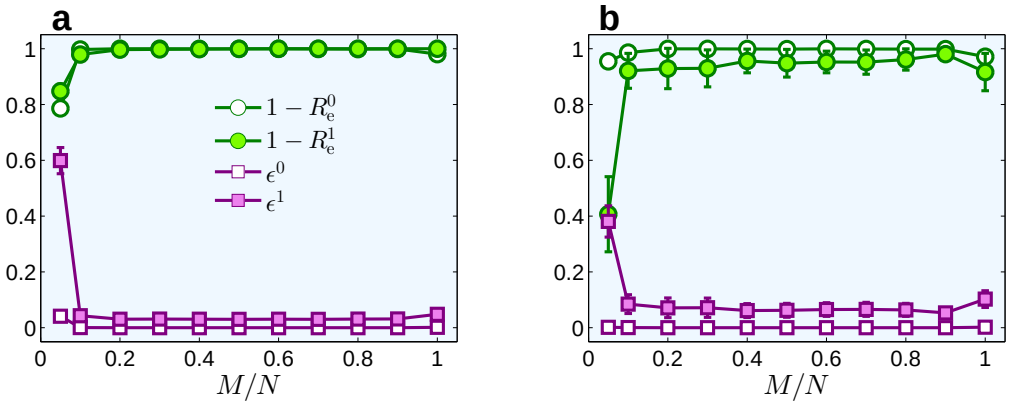

FIG. 3: Structural estimation success rates and parameter estimation errors versus the normalized data amount. For SDBM dynamics on (a) ER-random and (b) BA scale-free networks, the success rates of detection of existent links and identification of nonexistent links, $1-R_e^1$ (green circles) and $1-R_e^0$ (white circles), respectively, versus the normalized data amount M/N with error bars. The absolute values of the errors in estimating the link weights and the nodal biases for the existent links (purple squares) and non-existent links (white squares) are also shown. Most data points have quite small error bars, indicating the performance stability of our method. High performance structural and parameter estimations are achieved insofar as M/N exceeds about 10%.

measurements can be obtained. Overall, the equivalent SDBM correspondence holds and our reconstruction scheme for real world networks is effective.

C. Parameter estimation scheme

From the reconstructed network structure, any node i's k_i immediate neighbors, m_1, m_2, ..., m_{k_i}, and their state configuration, $\mathbf{X}_i^{\rm MB} = (x_{m_1}, x_{m_2}, \ldots, x_{m_{k_i}})^{\rm T}$, can be identified. Since the probability that i's state is 1 at the next time step depends only on i's immediate neighbors, $\mathbf{X}_i^{\rm R}(t)$ in Eq. (5) can be simplified to $\mathbf{X}_i^{\rm MB}(t)$, and Eq. (5) can be written as

$$P\{x_i(t+1)=1|\mathbf{X}_i^{\rm R}(t)\} = P\{x_i(t+1)=1|\mathbf{X}_i^{\rm MB}(t)\} = \frac{1}{1+\exp[\sum_{m=1}^{k_i} w_{im}x_m(t)+b_i]}. \quad (10)$$

Accordingly, Eq. (9) can be simplified as

$$\mathbf{Y}_{(k_i+1)\times 1}^{\rm MB} = \ominus_{(k_i+1)\times(k_i+1)}^{\rm MB} \cdot \mathbf{V}_{(k_i+1)\times 1}^{\rm MB},$$

i.e.,

$$\begin{pmatrix} \ln q_i(t_1) \\ \ln q_i(t_2) \\ \vdots \\ \ln q_i(t_{k_i+1}) \end{pmatrix} = \begin{pmatrix} \langle x_{m_1}(t_1)\rangle, & \langle x_{m_2}(t_1)\rangle, \ldots, & \langle x_{m_{k_i}}(t_1)\rangle, & 1 \\ \langle x_{m_1}(t_2)\rangle, & \langle x_{m_2}(t_2)\rangle, \ldots, & \langle x_{m_{k_i}}(t_2)\rangle, & 1 \\ \vdots & \vdots & \vdots & \vdots \\ \langle x_{m_1}(t_{k_i+1})\rangle, & \langle x_{m_1}(t_{k_i+1})\rangle, \ldots, & \langle x_{m_{k_i}}(t_{k_i+1})\rangle, & 1 \end{pmatrix} \begin{pmatrix} w_{im_1} \\ w_{im_2} \\ \vdots \\ w_{im_{k_i}} \\ b_i \end{pmatrix}, \quad (11)$$

TABLE I: Description of the 14 dynamical processes on model networks and the conditional probabilities. The quantity $P_i^{0\to1}$ or $P_i^{1\to0}$ is the probability that the state of node i (of degree k_i) becomes 1 at the next time step when its current state is 0, or vice versa, conditioned on its current neighboring state configuration. The number of i's neighbors in state 1 is n_i. (See Supplementary Note 1 for a detailed description of the dynamics and parameters for estimating the conditional probabilities $P_i^{0\to1}$ and $P_i^{1\to0}$.)

Category	Dynamics Type	$P_i^{0\to1}$	$P_i^{1\to0}$
I	SDBM	$\frac{1}{1+\exp[\sum_{j=1,j\neq i}^{N} w_{ij}x_j(t)+b_i]}$	$\frac{\exp[\sum_{j=1,j\neq i}^{N} w_{ij}x_j(t)+b_i]}{1+\exp[\sum_{j=1,j\neq i}^{N} w_{ij}x_j(t)+b_i]}$
II	Ising Glauber [47]	$\frac{1}{1+\exp[\frac{2J}{\kappa}(k_i-2n_i)]}$	$\frac{\exp[\frac{2J}{\kappa}(k_i-2n_i)]}{1+\exp[\frac{2J}{\kappa}(k_i-2n_i)]}$
	SQ-SG [48]	$\frac{1}{1+\exp[(rk_i-n_i)/\kappa]}$	$\frac{\exp[(rk_i-n_i)/\kappa]}{1+\exp[(rk_i-n_i)/\kappa]}$
	SQ-PDG [48]	$\frac{1}{1+\exp[(b-1)(k_i-n_i)/\kappa]}$	$\frac{\exp[(b-1)(k_i-n_i)/\kappa]}{1+\exp[(b-1)(k_i-n_i)/\kappa]}$
III	Minority game [49–53]	$\frac{k_i-n_i}{k_i}$	$\frac{n_i}{k_i}$
	Voter [54, 55]	$\frac{n_i}{k_i}$	$\frac{k_i-n_i}{k_i}$
	Majority vote [54, 55]	$\begin{cases} Q & \text{if } n_i < k_i/2 \\ 1/2 & \text{if } n_i = k_i/2 \\ 1-Q & \text{if } n_i > k_i/2 \end{cases}$	$\begin{cases} 1-Q & \text{if } n_i < k_i/2 \\ 1/2 & \text{if } n_i = k_i/2 \\ Q & \text{if } n_i > k_i/2 \end{cases}$
IV	Link-update voter [56, 57]	$\frac{n_i}{\langle k\rangle}$	$\frac{k_i-n_i}{\langle k\rangle}$
	Language model[58, 59]	$S(\frac{n_i}{k_i})^\alpha$	$(1-S)(\frac{k_i-n_i}{k_i})^\alpha$
	Kirman [60, 61]	c_1+dn_i	$c_2+d(k_i-n_i)$
V	CP [62, 63]	$\frac{n_i}{k_i}\lambda_i$	μ_i
	SIS [64–67]	$1-(1-\lambda_i)^{n_i}$	μ_i
VI	SG [68]	*	*
	PDG [69, 70]	*	*

where the k_i+1 linear equations uniquely solve $w_{im_1},\ldots,w_{im_{k_i}}$ and b_i simply via

$$\mathbf{V}^{\rm MB}_{(k_i+1)\times1} = [\ominus^{\rm MB}_{(k_i+1)\times(k_i+1)}]^{-1}\cdot\mathbf{Y}^{\rm MB}_{(k_i+1)\times1}.$$

Our parameter estimation formulation is illustrated schematically in Fig. 4(a).

For a particular neighboring state configuration of node i, $\mathbf{X}_i^{\rm MB}(t)$, its occurring frequency determines the precision in the estimation of $P\{x_i(t+1)|\mathbf{X}_i^{\rm MB}(t)\}\simeq\langle x_i(t+1)\rangle$,

TABLE II: Reconstruction error rates. For the same dynamical processes in Tab. I, the error rates (in percentages) in uncovering the existent and non-existent links, R_e^1 and R_e^0, respectively. ER-random and BA scale-free networks of size $N = 100$ and average degree $\langle k \rangle = 4$ are used as the underlining network supporting the various dynamical processes. The normalized number of measurements used in compressive sensing is $M/N = 0.4$ for all cases.

Category	Dynamics Type	R_e^0 / R_e^1 (%, ER)	R_e^0 / R_e^1 (%, BA)
I	SDBM	0.0 / 0.1	0.1 / 3.4
II	Ising Glauber [47]	0.0 / 0.0	0.0 / 0.0
	SQ-SG [48]	0.0 / 0.0	0.0 / 3.2
	SQ-PDG [48]	0.0 / 0.0	0.3 / 3.3
III	Minority game [49–53]	0.0 / 0.6	0.0 / 0.2
	Voter [54, 55]	0.0 / 0.0	0.0 / 0.0
	Majority vote [54, 55]	0.0 / 0.0	0.0 / 0.1
IV	Link-update voter [56, 57]	0.0 / 0.0	1.8 / 3.6
	Language model[58, 59]	0.0 / 0.0	0.0 / 0.4
	Kirman [60, 61]	0.0 / 2.3	0.0 / 3.8
V	CP [62, 63]	0.0 / 1.4	0.0 / 0.4
	SIS [64–67]	0.3 / 5.2	0.1 / 15.6
VI	SG [68]	0.0 / 1.7	0.0 / 9.4
	PDG [69, 70]	0.1 / 9.6	0.1 / 9.8

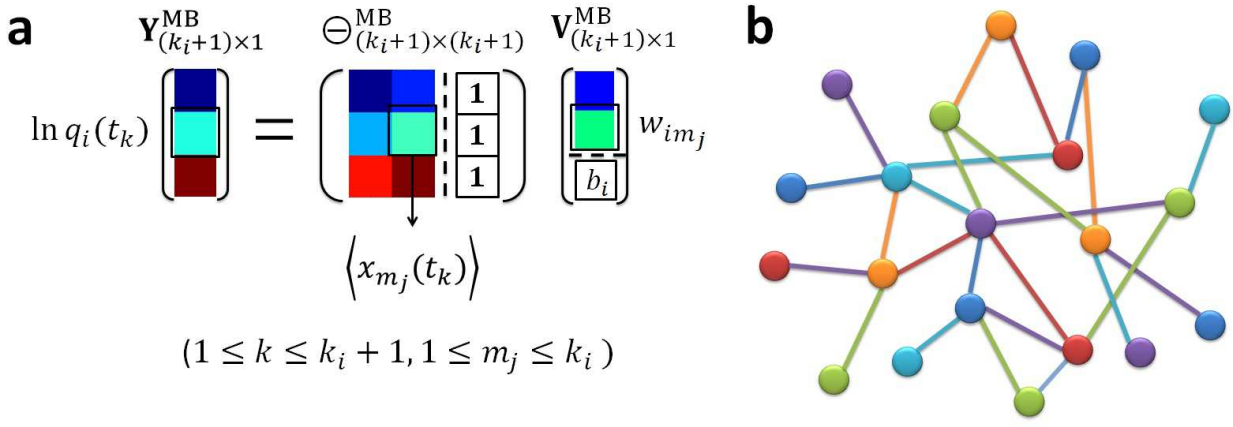

FIG. 4: A schematic illustration of SDBM parameter estimation. (a) For the SDBM of the same system in Fig. 1(a,b), the corresponding parameter estimation framework as in Eq. (11). The connections of the network have already been reconstructed, so the entries in Eq. (11) can be obtained from a node's Markov blanket [Fig. 1(b)]. The calculation is implemented for each node in the system. (b) The values of the link weights and the nodal biases (different colors) for the corresponding SDBM are calculated via the parameter estimation scheme in (a) and the degree guided solution substitution operation (see **Methods**).

which in turn determines the solution precision of Eq. (11). The occurrence of different neighboring state configurations for the same node may differ dramatically. Furthermore, the accuracy in estimating the probability $P\{x_i(t+1)|\mathbf{X}_i^{\rm MB}(t)\}$ depends on the node degree due to the increasing difficulty in finding exactly the same configurations for larger degree nodes. Overcoming the estimation difficulty is a highly non-trivial problem. Exploiting the available data further, we develop a degree guided solution-substitution operation to cope with this difficulty, where sufficient estimation precision is guaranteed for most cases (see **Methods**). A SDBM with estimated parameters is schematically shown in Fig. 4(b).

D. Universal dynamics approximator

In Table I, the complex network dynamics are categorized in terms of the specific probabilities $P_i^{0\to1}$ and $P_i^{1\to0}$. In particular, category I is for the SDBM dynamics and category II contains dynamical processes with $P_i^{0\to1}$ and $P_i^{1\to0}$ having a mathematical form similar to that of the SDBM. For category III, the forms of $P_i^{0\to1}$ and $P_i^{1\to0}$ for the three types of dynamics are quite different. Despite the differences among the dynamical processes in the three categories, they share a key property: i.e., $P_i^{0\to1}+P_i^{1\to0}=1$, which plays a critical role in implementing the parameter estimation algorithm. For the processes in categories IV and V, we have $P_i^{0\to1}+P_i^{1\to0}\neq1$, where $P_i^{1\to0}$ is a time-invariant constant for the nodal dynamics in category V.

We first test our parameter estimation scheme using the state time series generated by the SDBM, which can be validated through a direct comparison of the estimated parameter values with their true values, as shown in Figs. 2(a-c). However, since the parameters only affect the system collectively (not individually) in the form of the product summation [Eq. (5)] and our goal is to assess the predictive power, we introduce an alternative validation scheme. For each particular system configuration, the acceptable parameter estimation results would serve as a base to generate another SDBM with identical conditional probabilities for each node at each time step, as compared with those of the original system. (A visual comparison between the conditional probabilities of the original system and that generated via the reconstructed SDBM is presented in Supplementary Note 4). Figure 5(a) shows the error distributions of the estimated conditional probability time series, where an overwhelmingly sharp peak occurs at 0, indicating an excellent agreement between the estimated and the true parameter values.

For typical dynamical processes on complex networks, our goal is to find the equivalent SDBMs whose true parameter values are not available. In this case, the performance of the parameter estimation scheme can be assessed through the reconstructed conditional probabilities. Based on the recovered network structure, the time series of the network dynamics are fed into the parameter estimation scheme, and the link weights and the nodal biases are obtained to form a system obeying the SDBM dynamics. Corresponding to the categories in Table I, the distributions of the estimation errors between the original conditional probability $P\{x_i(t+1)=1|\mathbf{X}_i^{\rm R}(t)\}$ and the one generated by the newly constructed SDBM are shown in Fig. 5, where panels (a-f) show the error distributions corresponding to the six types of dynamics in categories II and III in Table I, respectively. In each case, a sharp peak at zero dominates the distribution, indicating the equivalence of the reconstructed SDBM to the original dynamics. Given a particular type of complex network dynamics, the SDBM

resulted from our structural and parameter estimation framework is indeed equivalent to the original dynamical system. The limited amount of data obtained from the original system renders important state prediction of the system, a task that can be accomplished by taking advantage of the equivalence of the SDBM to the original system in the sense that the SDBM produces approximately equal state transition probabilities in the immediate future, given the current system configuration. The SDBM thus possesses a significant predictive power for the original system. Regardless of the type of the dynamical process, insofar it satisfies the relation $P_i^{0\to1} + P_i^{1\to0} = 1$, the reconstructed SDBM can serve as a universal dynamics approximator.

For an SDBM, the relation $P_i^{1\to1} = 1 - P_i^{1\to0} = P_i^{0\to1}$ holds in general. However, for the dynamical processes in categories IV and V, we have $P_i^{1\to1} \neq 1 - P_i^{1\to0} = P_i^{0\to1}$ so that a single SDBM is not sufficient to fully characterize the dynamical evolution. Our solution is to construct two SDBMs, A and B, each associated with one of the two cases: $x_i(t) = 0$ and $x_i(t) = 1$, respectively. The link weights $w_{ij}^{\rm A}$ (or $w_{ij}^{\rm B}$) and the nodal bias $b_i^{\rm A}$ (or $b_i^{\rm B}$) for node i in SDBM A (or B) are computed for all the time steps t satisfying $x_i(t) = 0$ (or $x_i(t) = 1$), leading to $P\{x_i(t+1) = 1|\mathbf{X}_i^{\rm R}(t)\}$ for $x_i(t) = 0$ (or $x_i(t) = 1$) from SDBM A (or B). Using this strategy, the dominant peaks at zero persist in the error distributions for the dynamical processes in category IV, as shown in Figs. 5(g-i). For the epidemic spreading dynamics (CP and SIS) in category V, the fixed value of $P_i^{1\to0}$ for each node i can be acquired through $P_i^{1\to0} \simeq \langle x_i(t_1+1)\rangle_{t_1}$, where $\langle x_i(t_1+1)\rangle_{t_1}$ stands for the average of $x_i(t_1+1)$ over all values of t_1 satisfying $x_i(t_1) = 1$. Through this approach, SDBM B is in fact a network without links but with each node's bias satisfying $\mu_i = \exp(b_i)/[1+\exp(b_i)]$, where μ_i is node i's recovery rate. Figures 5(j) and 5(k) show the error distributions of the conditional probability recovery for the spreading processes, where we see that the errors are essentially zero. If the method of solving SDBM B in category IV is adopted to the dynamical processes in other categories, i.e., without any prior knowledge about $P_i^{1\to0}$, the resulted SDBM would have nearly identical link weight values with respect to SDBM A (in categories I-III) or have close-to-zero link weights and $\mu_i \simeq \exp(b_i)/[1+\exp(b_i)]$ for category V, despite that their conditional probability recovery errors may be slightly larger than those in Fig. 5. The persistent occurrence of a dominant peak at zero in the error distribution suggests the power of combined SDBMs as a universal dynamics approximator, regardless of the specifics of the transition probability. When limited prior knowledge about $P_i^{1\to0}$ is available, SDBM B can be simplified or even removed without compromising the estimation accuracy. In general, the universal approximator has a significant short-term predictive power for arbitrary types of dynamics on complex networks.

In the terminology of machine learning, the conditional probability recovery error is called the "training error," since it is obtained from the same data set used to build (or "train") the approximator. In machine learning, the data points generated from the same system that have not been used in the training process can be exploited to validate or test the actual performance of the trained model [32], which in our case is the approximator. As a result, the time series generated from the original complex network system after the approximator is built can be used as the test data set. (Absence of hyper-parameters in the reconstruction process means that cross validation is unnecessary.) In most cases, the training errors are generally smaller than the test errors, since the training data set is already well-fitted by the model (the approximator) in the training process, while the test data are new and may

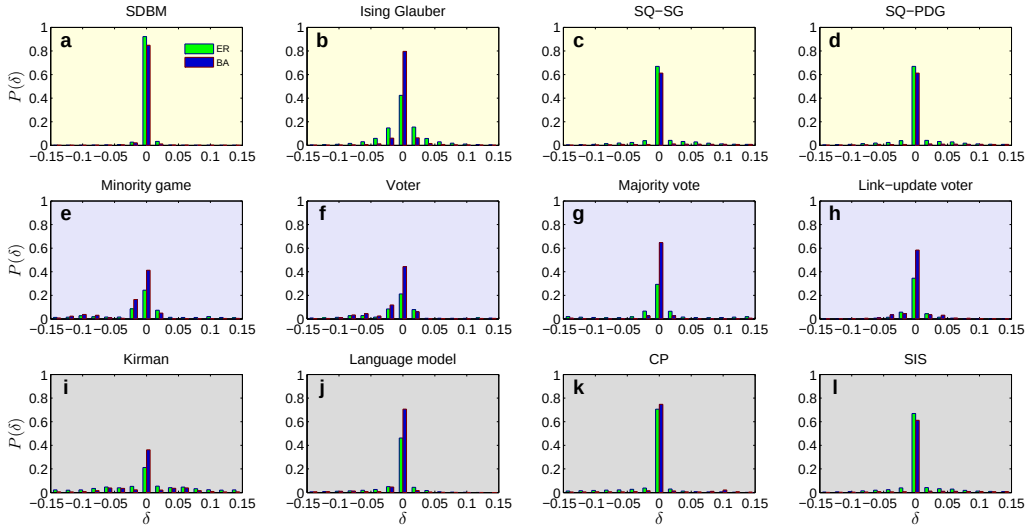

FIG. 5: Distributions of the conditional probability estimation errors for various complex network dynamics. The distributions of $\delta = |P\{x_i(t+1) = 1|\mathbf{X}_i^{\mathrm{R}}(t)\} - P^{\mathrm{est}}[x_i(t+1) = 1|\mathbf{X}_i^{\mathrm{R}}(t)]|$ for the dynamical processes in categories I to V from Table I for ER random (green bars) and BA scale-free (blue bars) networks, where $P^{\mathrm{est}}[x_i(t+1) = 1|\mathbf{X}_i^{\mathrm{R}}(t)]$ denotes the conditional probability estimated from the corresponding SDBM approximator through the original state configuration times series, where $1 \leq i \leq N$ and $1 \leq t \leq T$.

be out of the fitting range of the current model. Feeding the state configurations of the test data set into the approximator, we calculate the corresponding conditional probabilities using Eq. (5) and compare them to the true values. The results reveal a clear advantage of the approximator built from our scheme, i.e., the training and test errors are nearly identical, indicating the absence of any over-fitting issues that are common in various machine learning methodologies [32].

III. DISCUSSION

Reconstructing complex dynamical systems from data is a frontier field in network science and engineering with significant applications. Our study was motivated by the question: is it possible to build a universal "machine" to reconstruct, from data only, the underlying complex networked dynamical system and to make predictions? While this paper does not provide a mathematically rigorous solution, significant and (in some cases) striking results are obtained, which give strong credence that such a machine may be possible. In particular, we combine compressive sensing and machine learning to propose two concepts: universal network structural estimator and dynamics approximator. Universality is fundamentally possible due to the fact that many dynamical processes on complex networks are of the Markov type and the interactions among the nodes are local. As a result, utilizing basic tools from machine learning and statistical physics, one can build up an energy based Markov network model (e.g., a sparse dynamical Boltzmann machine) to construct a uni-

versal estimator and approximator for different types of complex network structures and dynamics. For a large number of representative dynamical processes studied in this paper, we demonstrate that such a universal SDBM can be reconstructed based on compressive sensing and the scheme of K-means using data only, without requiring any extra information about the network structure or the dynamical process. The working of the SDBM is demonstrated using a large number of combinations of the network structure and dynamics, including many real world networks and classic evolutionary game dynamics. An SDBM with its parameters given by the equations constructed from the times series along with the estimated network structure is able to reproduce the conditional probabilities quantitatively and, accordingly, it is capable of predicting the state configuration at least in a short term. We demonstrate that, for certain types of dynamics, the approximator can reproduce the dynamical process statistically, indicating the potential of its serving as a generative model for long term prediction in such cases (Supplementary Note 5).

While we assume binary dynamics, in principle the methodology can be applied to other types of dynamical processes. In particular, Eq. (4) can be readily extended to the conditional probability of each possible state value λ_j, i.e., $P\{x_i(t+1) = \lambda_j | \mathbf{X}_i^{\mathrm{R}}(t)\} = P\{x_i(t+1) = \lambda_j, \mathbf{X}_i^{\mathrm{R}}(t)\} / \sum_s P\{x_i(t+1) = \lambda_s, \mathbf{X}_i^{\mathrm{R}}(t)\}$. A potential difficulty is that the configuration space of the system states grows exponentially with the number of choices of λ_j so that, given a finite amount of data, the number of time instances corresponding to each particular configuration decreases exponentially, leading to a significant reduction in the estimation precision of the conditional probability.

Our effort represents an initial attempt to realize a universal estimator and approximator, and the performance of our method is quite competitive in comparison with the existing reconstruction schemes designed for specific types of dynamics, such as the compressive sensing technique for evolutionary game and epidemic spreading dynamics [27–31], as well as methods adopting the Bethe approximation, pseudo-likelihood, mean-field theory, and decimation operation for static and kinetic inverse Ising problems [9–20]. In realistic applications, the data obtained may be discontinuous or incomplete. In such cases, the short-term predictive power possessed by the universal estimator and approximator can be exploited to overcome the difficulty of missing data, as the Markov network nature of the SDBM makes backward inference possible so that the system configurations during the time periods of missing data may be inferred. When long term prediction is possible, the universal approximator has the critical capability of simulating the system behavior and predicting the chance that the system state enters into a global absorption phase, which may find significant applications such as disaster early warning. Another interesting reverse-engineering problem lies in the mapping between the original dynamics and the corresponding parameter value distribution of the reconstructed SDBM. That is, a certain parameter distribution of the SDBM may indicate a specific type of the original dynamics. As such, the correspondence can be used for precisely identifying nonlinear and complex networked dynamical systems. It is also possible to assess the relative importance of the nodes and links in a complex network based on their corresponding biases and weights in the reconstructed SDBM for controlling the network dynamics. These advantages justify our idea of developing a universal machine for data-based reverse engineering of complex networked dynamical systems, calling for future efforts in this emerging direction to further develop and perfect the universal network structural estimator and dynamics approximator.

IV. METHODS

Structural estimation details. For each type of dynamics, 10 different network realizations are generated for both BA scale-free and ER random topologies. For any node in a particular network realization, the corresponding connection weight vector $\mathbf{V}_{N\times 1}$ is obtained by averaging over 100 compressive sensing implementations. The elements corresponding to the existent nodes are distinguished from the non-existent links by feeding the averaged $\mathbf{V}_{N\times 1}$ into the K-means algorithm (see below). The unweighted adjacency matrix is then obtained.

Conflict resolution. Since the links are bidirectional, the node on each side provides a weighted solution of the same link. The two solutions may be quite different, giving contradictory indication of the existence of the link and resulting in an asymmetric adjacency matrix. For majority types of dynamical processes on complex networks, compressive sensing almost always gives higher prediction accuracy for lower degree nodes due to their connection sparsity, which holds true especially for nodes with their degrees smaller than the network average. Based on this fact, when encountering contradictory solutions, we determine the link existence by examining the lower degree side if the degree value is equal to or smaller than the network average. For cases where the degrees of both sides are larger than the network average, we find that the false negative rates are often high. This is because compressive sensing tends to give over simplified results such as inducing a more than necessary level of sparsity to the solution or causing large fluctuations with the non-existent links so they are mixed up with the existent ones. As a result, contradictory solutions are treated as positive (existent) solutions. For two types of dynamics, the SDBM dynamics and link-update voter dynamics, or dynamics on real world networks, treating all contradictory solutions this way, regardless of degree values, can improve the reconstruction precision, albeit only slightly in some cases.

Implementation of the K-means algorithm. K-means is one of the simplest and most popular clustering algorithms, which has been used widely for unsupervised clustering tasks [32]. It provides each data example an assignment to a cluster within which the data examples are relatively close (or similar) while being distant from the ones in other clusters. The main steps for solving a typical two-dimensional data clustering problem via K-means are schematically illustrated in Fig. 6. For each vector $\mathbf{V}_{N\times 1}$ obtained from averaging over multiple applications of compressive sensing, picking out the elements corresponding to the existent links from the non-existent ones with their fluctuating element values is equivalent to a one-dimensional clustering problems with two target clusters, which is one dimension lower than the case shown in Fig. 6. When implementing the K-means algorithm, we choose the initial cluster center positions for the two clusters as the maximum and minimum values of the vector elements with the bias b_i excluded. This is justified because the compressive sensing solution of b_i can have an overwhelmingly high absolute value, which does not provide any structural information but can severely disrupt the clustering process, as demonstrated in Figs. 2(d,f). Due to the sparsity of complex networks, the cluster with smaller number of components is regarded as containing the solutions of the existent links, and the components of the other one correspond to the non-existent links.

Link weights and nodal bias estimation. For each node i, we rank the occurrences of all the existing configurations of its neighbor's states. Among the top ones, $k_i + 1$ are selected

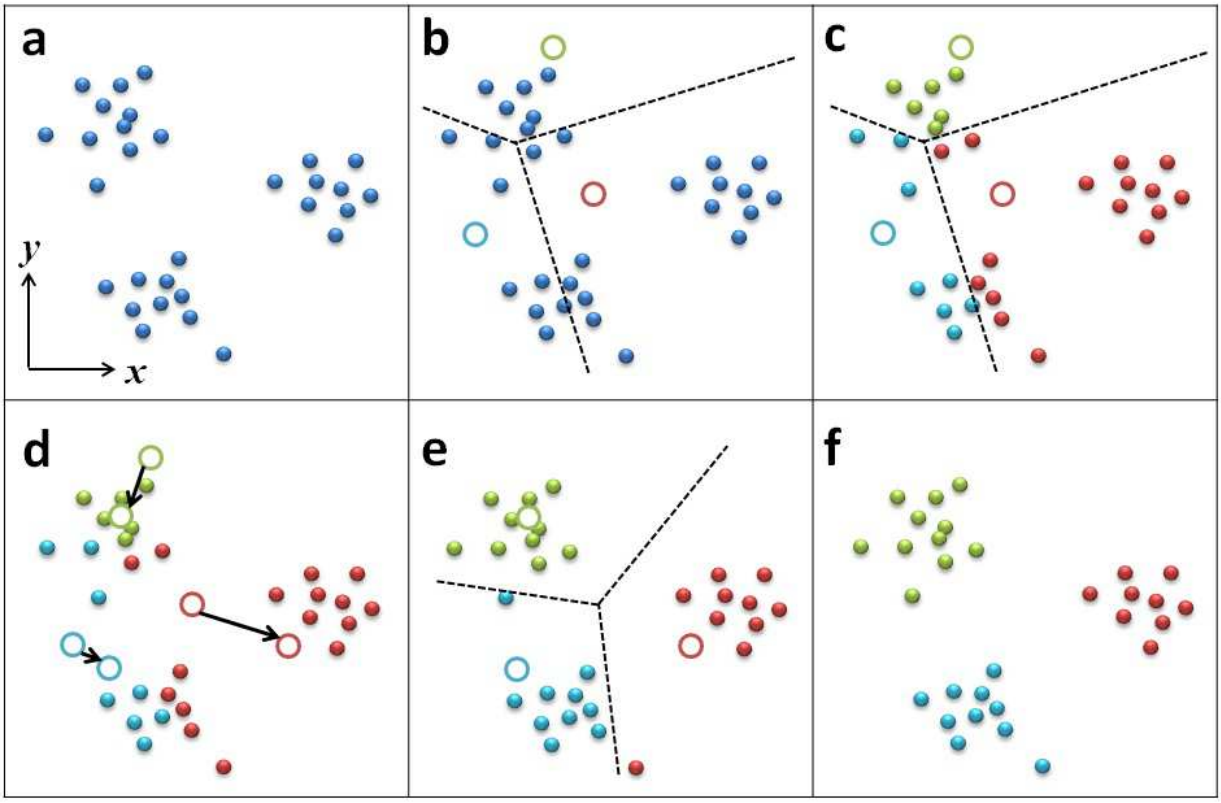

FIG. 6: A schematic illustration of the K-means algorithm for two-dimensional data clustering. (a) The data points (solid blue circles) to be clustered in a 2D feature space. There are three clusters, so $K = 3$. The K-means algorithm is capable of assigning each data point into one of the clusters. (b) For random locations of the cluster centers (aqua, green, and red hollow circles), each data point can be associated with the closest center. (c) The 2D space is divided into three regions through three decision boundaries (black dashed lines), each containing the corresponding data points whose closest center is within. The data points currently in the regions with the aqua, green, and red centers are assigned to the corresponding clusters, respectively. At this stage, data points may be assigned to a cluster that did not belong to the one at the beginning of the process. (d) Each center moves to the centroid of the data points currently assigned to it (movements shown by the black arrows). (e) The updated cluster assignments of the data points are obtained according to the new center locations. The steps in (c) and (d) are repeated until convergence is achieved. (f) The final cluster assignments. Different from this illustration, the compressive sensing solutions of the link weights w_{ij} are one-dimensional data points, which form two clusters in 1D, corresponding to the existent and non-existent links, respectively. (For better visualization, we use the 2D case to illustrate the K-means algorithm instead of 1D.)

to ensure that the coefficient matrix $\ominus^{\rm MB}_{(k_i+1)\times(k_i+1)}$ on the right hand side of Eq. (11) has full rank so that the solutions, $w_{im_1}, w_{im_2}, \ldots, w_{im_{k_i}}, b_i$, are unique (the selected configurations are not necessarily on the exact top, since the real top $k_i + 1$ ones may not provide a full rank coefficient matrix).

Due to insufficient number of samples or some particular features of a specific dynamical process, $\langle x_i(t+1)\rangle$, the statistical estimation of $P\{x_i(t+1)|\mathbf{X}_i^{\rm MB}(t)\}$ (or $P\{x_i(t+1)|\mathbf{X}_i^{\rm R}(t)\}$),

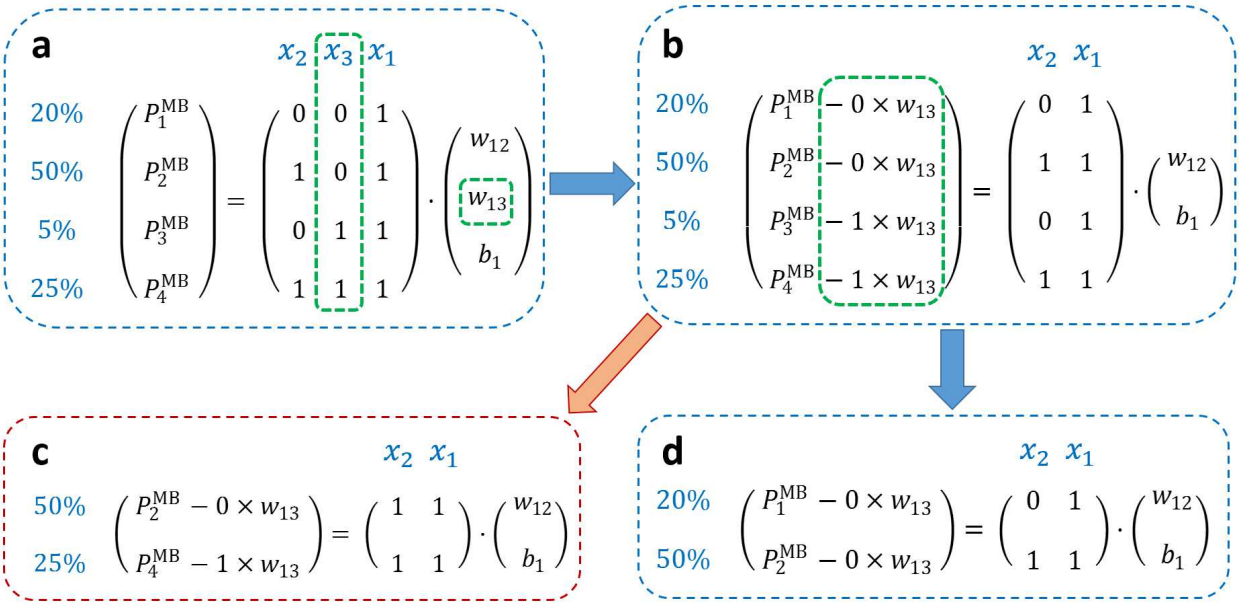

FIG. 7: An example of our proposed degree guided solution-substitution operation and final equation group construction. The target node 1 has only two neighbors, nodes 2 and 3. Without loss of generality, we set $k_3 < k_1 = 2 < k_2$ so that the link weight between nodes 1 and 3, w_{13}, is already obtained. The quantity $P_s^{\rm MB} = \ln(1/\langle x_1(t+1)\rangle_s - 1)$ ($s = 1, \ldots, 4$, as there are $2^{k_1} = 4$ possible (x_2, x_3) configurations in total) denotes the estimated probability for $x_1 = 1$ under configuration s at the next time step. The occurring probabilities of the corresponding (x_2, x_3) configurations are listed as percentages in the left column of each panel. (**a**) All four (x_2, x_3) configurations are shown by the first two columns of the 4×3 matrix in the equation. (**b**) The contribution of the known w_{13} and the configurations of x_3 as marked in (**a**) are moved to the left-hand side of the equation. (**c**) In order to solve for $(w_{12}, b_1)^{\rm T}$, the two most precise $P_s^{\rm MB}$ values ($s = 2$ and 4) corresponding to the most frequent (x_2, x_3) configurations from (**b**) are chosen to build a linear 2-equation group. However, the 2×2 matrix on the right-hand side does not have full rank and, hence, this equation group is ill defined (**d**) Configurations $s = 1$ and 2 are selected to construct a 2-equation group with a full rank 2×2 matrix on the right-hand side and relatively precise probability estimations, and this equation group is used to solve $(w_{12}, b_1)^{\rm T}$.

can be 0 or 1, which respectively makes $1/\langle x_i(t+1)\rangle$ or $\ln[1 - 1/\langle x_i(t+1)\rangle]$ in Eqs. (9) and (11) diverge. Without loss of generality, we set $\langle x_i(t+1)\rangle = \epsilon$ (or $\langle x_i(t+1)\rangle = 1 - \epsilon$) if $\langle x_i(t+1)\rangle = 0$ (or 1), where ϵ is a small positive constant.

For node i of degree k_i, the total number of the possible neighboring state configurations is 2^{k_i}, so large degree nodes have significantly more configurations. The process may then regard every particular type of configurations as useful and accordingly lead to inaccurate estimate of $P\{x_i(t+1)|\mathbf{X}_i^{\rm MB}(t)\}$. Our computations show that properly setting a tolerance in the Hamming distance that allows similar but not exactly identical configurations to be treated as the same $\mathbf{X}_i^{\rm MB}(t)$ can improve the estimation performance. For a particular neighboring state configuration with too fewer identical matches in the observed data, configurations with difference in one or more digits in the Hamming distance are used instead, until a sufficient number of matches are found. For nodes of degrees larger than, say 15, the Hamming distance tolerances within 2 or 3 usually lead to a reasonable number of matches

for estimating $P\{x_i(t+1)|\mathbf{X}_i^{\mathrm{MB}}(t)\}$. Extensive calculation shows that the small inaccuracy has little effect on the reconstruction accuracy.

Degree guided solution-substitution operation. For node i's neighbors, the occurrence frequency of a particular state configuration is generally higher for smaller values of k_i. Accordingly, the probability estimation conditioned on this configuration can be more accurate for smaller values of k_i. More precise conditional probabilities in turn lead to a higher estimation accuracy of link weights and node biases. Similar to resolving the solution contradiction in the structural reconstruction step, for a pair of linked nodes, i and j of different degrees, w_{ij} solved from the equation group of node i is likely to be more accurate than w_{ji} obtained via node j, if $k_i < k_j$, even ideally they should have the identical values. As a result, using the solution obtained from a lower degree node as the value of the link weight provides a better estimation. We run the calculation for all nodes in the network one by one in a degree-increasing order so that the link weights of the smallest degree nodes are acquired earlier than for other nodes. For the larger degree nodes, the link weights shared with the smaller degree nodes are substituted by the previously obtained values, which are treated as known constants instead of variables waiting to be solved. This operation effectively removes the contribution of the lower degree neighbors from the equation and so reduces the number of unknown variables. A reduced equation group in a form similar to Eq. (11) can be built up based on the most frequently occurring state configurations of the remaining neighbors. When the full-rank condition is met, maximum possible precision of the remaining unknown link weights can be achieved. Consequently, with the substitution operation, the k_i link weights of node i, which can be inaccurate if solved from the original k_i+1-equation group, can be estimated with the maximum possible accuracy. An example of this substitution operation and the final equation group construction process is shown in Fig. 7.

Our calculations show that the application of the degree guided solution-substitution operation can significantly increase the accuracy of the estimation of the link weights and nodes biases. This operation is thus key to making the SDBM correspondence a reliable approximator of the original network dynamics.

As shown in Fig. 5, for dynamical processes in categories I and II, the estimation errors are dominantly distributed at zero. For processes in other categories, besides the dominant peak at zero, there exist multiple small peaks at nonzero error values. These small side peaks are a consequence of the model complexity of the Markov networks.

Model complexity and representation power. For dynamical processes in categories I and II, the transition probabilities $P_i^{0\to1}$ all have the form $1/[1+\exp(An_i+Bk_i)]$, where A and B are constants, and n_i denotes the number of node i's neighbors whose states are 1. We have

$$[1+\exp(An_i+Bk_i)]^{-1}=\{1+\exp[\sum_{m=1}^{k_i}w_{im}x_m(t)+b_i]\}^{-1},$$

which gives

$$\sum_{m=1}^{k_i}Ax_m(t)+Bk_i=\sum_{m=1}^{k_i}w_{im}x_m(t)+b_i. \tag{12}$$

In the ideal case where an absolutely accurate estimate of $P\{x_i(t+1)=1|\mathbf{X}_i^{\mathrm{R}}(t)\}$ can be obtained, Eq. (12) holds for any possible neighboring state configurations. We thus have

$w_{im} = A$ and $b_i = Bk_i$, and the probabilities conditioned on these configurations sharing the same values of n_i in the approximator are all equal to $P_i^{0\to1}$. This means that, in theory, the conditional probabilities can be reconstructed with zero errors. In fact, a one-to-one mapping between the coefficients indicates that the model complexity of the SDBM provides the approximator with sufficient representation power to model the dynamics processes in categories I and II. Practically, since the statistical estimations of $P\{x_i(t+1) = 1|\mathbf{X}_i^{\mathrm{R}}(t)\}$ may not be absolutely identical under different neighboring configurations with the same values of n_i due to random fluctuations, we have $w_{im} \approx A$ so that the conditional probabilities generated by the approximator may differ from each other slightly and also from the true probability $P_i^{0\to1}$. As a result, random recovery errors can occur.

For dynamical processes in categories other than I and II, the simple coefficient-mapping relation between the corresponding $x_m(t)$ terms on the two sides of Eq. (12) become nonlinear, due to the fact that the specific forms of $P_i^{0\to1}$ differ substantially from that of the SDBM. In this case, each particular neighboring state configuration produces a distinct equation. There are 2^{k_i} equations in total, while the number of unknown variables to be solved is only $k_i + 1$ (w_{im} for $m = 1, \ldots, k_i$ and b_i). For $k_i \geq 2$, there are thus more equations than the number of unknown variables. As a result, the representation power of the SDBM approximator is limited by its finite model complexity so that, even in principle, the approximator may not be able to fully describe the original dynamical process. In our framework, we calculate the Markov link weights and the node biases according to the k_i+1 most frequently appeared neighboring state configurations. A consequence is that imprecise conditional probability estimations can arise for the configurations with relatively lower occurring frequency, giving rise to the nonzero peaks in the error distribution in Fig. 5. However, interestingly, with respect to the precision of the conditional probabilities produced by the approximator, the SDBM parameters do not show a significantly strong preference towards the most frequently occurring configurations. In practice, the estimated conditional probabilities for the majority of the less frequently occurring configurations also fall within a close range of the true values. This phenomenon suggests the power of the approximator to work beyond the limit set by its theoretical model complexity. This is the main reason for the emergence and persistence of the dominant peak at zero in the error distribution.

---

[1] Grün, S., Diesmann, M. & Aertsen, A. Unitary events in multiple single-neuron activity: I. detection and significance. *Neural Comput.* **14**, 43 (2002).

[2] Grün, S., Aertsen, A. & Rotter, S. Statistical significance of coincident spikes: Count-based versus rate-based statistics. *Neural Comput.* **14**, 121 (2002).

[3] Pipa, G. & Grün, S. Nonparametric significance estimation of joint-spike events by shuffling and resampling. *Neurocomputing* **52-54**, 31 (2003).

[4] Gardner, T. S., di Bernardo, D., Lorenz, D. & Collins, J. J. Inferring genetic networks and identifying compound mode of action via expression profiling. *Science* **301**, 102 (2003).

[5] Bansal, M., Belcastro, V., Ambesi-Impiombato, A. & di Bernardo, D. How to infer gene networks from expression profiles. *Mol. Syst. Biol.* **3**, 78 (2007).

[6] Geier, F., Timmer, J. & Fleck, C. Reconstructing gene-regulatory networks from time series, knock-out data, and prior knowledge. *BMC Syst. Biol.* **1**, 11 (2007).

[7] Supekar, K., Menon, V., Rubin, D., Musen, M. & Greicius, M. D. Network analysis of intrinsic functional brain connectivity in alzheimers disease. *PLoS Comput. Biol.* **4**, e1000100 (2008).

[8] Hecker, M., Lambeck, S., Toepferb, S., van Someren, E. & Guthke, R. Gene regulatory network inference: Data integration in dynamic modelsa review. *BioSystems* **96**, 86 (2009).

[9] Tanaka, T. Mean-field theory of boltzmann machine learning. *Phys. Rev. E* **58**, 2302 (1998).

[10] Cocco, S. & Monasson, R. Adaptive cluster expansion for inferring boltzmann machines with noisy data. *Phys. Rev. Lett.* **106**, 090601 (2011).

[11] Aurell, E. & Ekeberg, M. Inverse ising inference using all the data. *Phys. Rev. Lett.* **108**, 090201 (2012).

[12] Nguyen, H. C. & Berg, J. Mean-field theory for the inverse ising problem at low temperatures. *Phys. Rev. Lett.* **109**, 050602 (2012).

[13] Ricci-Tersenghi, F. The bethe approximation for solving the inverse ising problem: a comparison with other inference methods. *J. Stat. Mech.* **2012**, 08015 (2012).

[14] Roudi, Y. & Hertz, J. Mean field theory for nonequilibrium network reconstruction. *Phys. Rev. Lett.* **106**, 048702 (2011).

[15] Méard, M. & Sakellariou, J. Exact mean-field inference in asymmetric kinetic ising systems. *J. Stat. Mech.* **2011**, 08015 (2011).

[16] Sohl-Dickstein, J., Battaglino, P. B. & DeWeese, M. R. New method for parameter estimation in probabilistic models: Minimum probability flow. *Phys. Rev. Lett.* **107**, 220601 (2011).

[17] Zhang, P. Inference of kinetic ising model on sparse graphs. *J. Stat. Phys.* **148**, 502–512 (2012).

[18] Zeng, H.-L., Alava, M., Aurell, E., Hertz, J. & Roudi, Y. Maximum likelihood reconstruction for ising models with asynchronous updates. *Phys. Rev. Lett.* **110**, 210601 (2013).

[19] Barnett, L., Lizier, J. T., Harré, M., Seth, A. K. & Bossomaier, T. Information flow in a kinetic ising model peaks in the disordered phase. *Phys. Rev. Lett.* **111**, 177203 (2013).

[20] Decelle, A. & Ricci-Tersenghi, F. Pseudolikelihood decimation algorithm improving the inference of the interaction network in a general class of ising models. *Phys. Rev. Lett.* **112**, 070603 (2014).

[21] Timme, M. Revealing network connectivity from response dynamics. *Phys. Rev. Lett.* **98**, 224101 (2007).

[22] Bongard, J. & Lipson, H. Automated reverse engineering of nonlinear dynamical systems. *Proc. Natl. Acad. Sci. U.S.A.* **104**, 9943 (2007).

[23] Shandilya, S. G. & Timme, M. Inferring network topology from complex dynamics. *New J. Phys.* **13**, 013004 (2011).

[24] Clauset, A., Moore, C. & Newman, M. E. J. Hierarchical structure and the prediction of missing links in networks. *Nature (London)* **453**, 98 (2008).

[25] Levnajić, Z. & Pikovsky, A. Network reconstruction from random phase resetting. *Phys. Rev. Lett.* **107**, 034101 (2011).

[26] Wang, W.-X., Yang, R., Lai, Y.-C., Kovanis, V. & Harrison, M. A. F. Time-series based prediction of complex oscillator networks via compressive sensing. *Europhys. Lett.* **94**, 48006 (2011).

[27] Wang, W.-X., Lai, Y.-C., Grebogi, C. & Ye, J.-P. Network reconstruction based on evolutionary-game data via compressive sensing. *Phys. Rev. X* **1**, 021021 (2011).

[28] Shen, Z., Wang, W.-X., Fan, Y., Di, Z. & Lai, Y.-C. Reconstructing propagation networks

with natural diversity and identifying hidden sources. *Nat. Commun.* **5**, 4323 (2014).

[29] Han, X., Shen, Z., Wang, W.-X. & Di, Z. Robust reconstruction of complex networks from sparse data. *Phys. Rev. Lett.* **114**, 028701 (2015).

[30] Wang, W.-X., Chen, Q.-F., Huang, L., Lai, Y.-C. & Harrison, M. A. F. Scaling of noisy fluctuations in complex networks and applications to network prediction. *Phys. Rev. E* **80**, 016116 (2009).

[31] Ren, J., Wang, W.-X., Li, B. & Lai, Y.-C. Noise bridges dynamical correlation and topology in coupled oscillator networks. *Phys. Rev. Lett.* **104**, 058701 (2010).

[32] Bishop, C. M. *Pattern Recognition and Machine Learning* (springer, 2006).

[33] Russell, S. & Norvig, P. *Artificial Intelligence: A Modern Approach (3rd Edition)* (Prentice Hall, 2009), 3 edn.

[34] Ackley, D. H., Hinton, G. E. & Sejnowski, T. J. A learning algorithm for boltzmann machines. *Cogn. Sci.* **9**, 147–169 (2014).

[35] Candès, E. J., Romberg, J. K. & Tao, T. Robust uncertainty principles: Exact signal reconstruction from highly incomplete frequency information. *IEEE Trans. Info. Theo.* **52**, 489–509 (2006).

[36] Candes, E. J., Romberg, J. K. & Tao, T. Stable signal recovery from incomplete and inaccurate measurements. *Commun. Pure Appl. Math.* **59**, 1207–1223 (2006).

[37] Donoho, D. L. Compressed sensing. *IEEE Trans. Info. Theo.* **52**, 1289–1306 (2006).

[38] Baraniuk, R. G. Compressive sensing. *IEEE Sig. Proc. Mag.* **24**, 118–121 (2007).

[39] Candès, E. J. & Wakin, M. B. An introduction to compressive sampling. *IEEE Sig. Proc. Mag.* **25**, 21–30 (2008).

[40] Romberg, J. Imaging via compressive sampling. *IEEE Sig. Proc. Mag.* **25**, 14–20 (2008).

[41] Su, R.-Q., Ni, X., Wang, W.-X. & Lai, Y.-C. Forecasting synchronizability of complex networks from data. *Phys. Rev. E* **85**, 056220 (2012).

[42] Su, R.-Q., Wang, W.-X. & Lai, Y.-C. Detecting hidden nodes in complex networks from time series. *Phys. Rev. E* **85**, 065201R (2012).

[43] Su, R.-Q., Lai, Y.-C., Wang, X. & Do, Y.-H. Uncovering hidden nodes in complex network in the presence of noise. *Sci. Rep.* **4**, 3944 (2014).

[44] Kishore, V., Santhanam, M. S. & Amritkar, R. E. Extreme events on complex networks. *Phys. Rev. Lett.* **106**, 188701 (2011).

[45] Chen, Y.-Z., Huang, Z.-G. & Lai, Y.-C. Controlling extreme events on complex networks. *Sci. Rep.* **4**, 06121 (2014).

[46] Chen, Y.-Z. *et al.* Extreme events in multilayer, interdependent complex networks and control. *Sci. Rep.* **5**, 17277 (2015).

[47] Glauber, R. J. Time-dependent statistics of the ising model. *J. Math. Phys. (N.Y.)* **4**, 294 (1963).

[48] Gao, K., Wang, W.-X. & Wang, B.-H. Self-questioning games and ping-pong effect in the ba network. *Physica A* **380**, 528–538 (2007).

[49] Challet, D. & Zhang, Y.-C. Emergence of cooperation and organization in an evolutionary game. *Physica A* **246**, 407–418 (1997).

[50] Challet, D., Marsili, M. & Zhang, Y.-C. Minority games: interacting agents in financial markets. *OUP Catalogue* (2013).

[51] Paczuski, M., Bassler, K. E. & Corral, A. Self-organized networks of competing boolean

agents. *Phys. Rev. Lett.* **84**, 3185–3188 (2000).

[52] Zhou, T., Wang, B.-H., Zhou, P.-L., Yang, C.-X. & Liu, J. Self-organized boolean game on networks. *Phys. Rev. E* **72**, 046139 (2005).

[53] Huang, Z.-G., Zhang, J.-Q., Dong, J.-Q., Huang, L. & Lai, Y.-C. Emergence of grouping in multi-resource minority game dynamics. *Sci. Rep.* **2**, 703 (2012).

[54] Liggett, T. M. *Interacting Particle Systems* (Springer, New York, 1985).

[55] de Oliveira, M. J. Isotropic majority-vote model on a square lattice. *J. Stat. Phys.* **66**, 273 (1992).

[56] Barrat, A., Barthélemy, M. & Vespignani, A. *Dynamical Processes on Complex Networks* (Cambridge University Press, Cambridge, England, 2008).

[57] Castellano, C., Fortunato, S. & Loreto, V. Statistical physics of social dynamics. *Rev. Mod. Phys* **81**, 591 (2009).

[58] Vazquez, F., Castelló, X. & Miguel, M. S. Agent based models of language competition: Macroscopic descriptions and order-disorder transitions. *J. Stat. Mech.* **04**, 04007 (2010).

[59] Abrams, D. M. & Strogatz, S. H. Modelling the dynamics of language death. *Nature (London)* **424**, 900 (2003).

[60] Kirman, A. Ants, rationality, and recruitment. *Quar. J. Econo.* **108**, 137 (1993).

[61] Alfarano, S., Lux, T. & Wagner, F. Estimation of agent-based models: The case of an asymmetric herding model. *Comp. Econo.* **26**, 19 (2005).

[62] Castellano, C. & Pastor-Satorras, R. Non-mean-field behavior of the contact process on scale-free networks. *Phys. Rev. Lett.* **96**, 038701 (2006).

[63] Volz, E. & Meyers, L. A. Epidemic thresholds in dynamic contact networks. *J. R. Soc. Interface* **6**, 233–241 (2009).

[64] Bailey, N. T. J. *The Mathematical Theory of Infectious Diseases* (Griffin, London, 1975).

[65] Anderson, R. M. & May, R. M. *Infectious Diseases in Humans* (Oxford University Press, Oxford, England, 1992).

[66] Pastor-Satorras, R. & Vespignani, A. Epidemic spreading in scale-free networks. *Phys. Rev. Lett.* **86**, 3200–3203 (2001).

[67] Pastor-Satorras, R. & Vespignani, A. Epidemic dynamics and endemic states in complex networks. *Phys. Rev. E* **63**, 066117 (2001).

[68] Sugden, R. *The Economics of Rights Co-operation and Welfare* (Blackwell, Oxford, UK, 1986).

[69] Axelrod, R. & Hamilton, W. D. The evolution of cooperation. *Science* **211**, 4489 (1981).

[70] Szabó, G. & Tőke, C. Evolutionary prisoners dilemma game on a square lattice. *Phys. Rev. E* **58**, 69 (1998).

ACKNOWLEDGEMENTS

This work was supported by ARO under Grant No. W911NF-14-1-0504 and by NSF under Grant No. 1441352.

AUTHOR CONTRIBUTIONS

Y.-Z.C. and Y.-C.L. designed research; Y.-Z.C. performed research; both analyzed data; Y.-C.L. and Y.-Z.C. wrote the paper.

ADDITIONAL INFORMATION

Competing financial interests: The authors declare no competing financial interests.